JOURNAL OF CATALYSIS 96, 574–585 (1985)

Propylene Hydroformylation on Rhodium Zeolites X and Y

II. *In Situ* Fourier Transform Infrared Spectroscopy

EDWARD J. RODE, MARK E. DAVIS,[1] BRIAN E. HANSON*

*Departments of Chemical Engineering and *Chemistry, Virginia Polytechnic Institute and State University, Blacksburg, Virginia 24061*

Received May 3, 1985; revised August 6, 1985

In situ Fourier transform infrared spectroscopy studies of carbonyl formation and propylene hydroformylation by RhNaX and RhNaY are reported. Rhodium dicarbonyl is formed on NaX. Two dicarbonyl species are present on NaY if the zeolite is dried prior to exposure of carbon monoxide. If the NaY is not dried, $Rh_6(CO)_{16}$ is ultimately formed. Propylene hydroformylation is shown to be proceeding similarly on RhNaX and RhNaY in homogeneous-like reaction pathways by comparing the *in situ* infrared spectra taken under hydroformylation conditions to data from solution. The selective poisoning of a RhNaY catalyst is consistent with hydroformylation active sites located on the surface of the zeolite particles.

INTRODUCTION

Infrared spectroscopy has played a major role in the study of rhodium-exchanged zeolites as catalysts for methanol carbonylation (*1–12*) and the hydroformylation of olefins (*13–15*). While the majority of catalytic studies employ IR as a tool to examine the catalyst before and after reaction, it is advantageous to perform *in situ* flow experiments. Yamanis *et al.* (*8*) have used this technique to help elucidate the mechanism for methanol carbonylation on RhNaX. Also, some reports have appeared which deal simply with the deposition of rhodium clusters onto different supports (*16, 17*), and the formation of rhodium carbonyls (*18, 19*) and rhodium carbonyl phosphines (*19*) on zeolites.

Both NaX and NaY zeolites have been used as supports for rhodium-catalyzed carbonylation and hydroformylation. Following a variety of pretreatments, the geminal dicarbonyl, $Rh(I)(CO)_2$–NaX was formed (*5, 8, 13, 19*). However, for NaY, both the $Rh(I)(CO)_2$–NaY (*9, 14, 18*) and the cluster, $Rh_6(CO)_{16}$–NaY (*13, 15*) have been observed. Lefebvre and Ben Taarit (*20*) and Shannon *et al.* (*21*) postulated that the $Rh(I)(CO)_2$–NaY consisted of two structures: $Rh(I)(CO)_2(O_z)_2$ with characteristic IR frequencies of 2101 and 2022 cm^{-1}, and $Rh(I)(CO)_2(O_z)(H_2O)$ with characteristic IR frequencies of 2116 and 2048 cm^{-1}, where O_z denotes zeolite framework oxygen. The objective of this investigation was to study rhodium carbonyl formation and propylene hydroformylation by RhNaX and RhNaY with *in situ* FTIR. Rhodium carbonyl formation and reactions with phosphines are presented in the first portion of this report. The second portion is devoted to the identification and location of propylene hydroformylation reaction intermediates. These results will be discussed in light of the catalytic activity data presented in our accompanying report (*22*).

EXPERIMENTAL

The materials and preparation of the catalysts are given elsewhere (*22*).

Infrared spectra were recorded on an IBM IR/32 spectrometer. All spectra have a resolution of 2 cm^{-1}. The flow IR cell is a modified version of the design described by Hicks *et al.* (*23*). The optical path length

[1] To whom correspondence should be addressed.

0021-9517/85 $3.00

was 1.5 mm. The catalyst was sieved to less than 325 mesh, and a $\frac{3}{8}$-in. diameter self-supporting wafer was formed by pressing to 30,000 psi. The catalyst wafer density was approximately 5 mg/cm^2; the wafers were approximately 0.1 mm thick. Irtran-2 windows were used. The cell also features a 3-way valve at the cell inlet which allowed for injections of liquids and gases. Complete details of the system are given elsewhere (*24*).

Pretreatment of the catalysts followed the same procedures outlined in our accompanying report (*22*). Reaction conditions were 3 : 3 : 2 : 1 propylene/hydrogen/nitrogen/carbon monoxide at 45 ml (STP)/min at ambient pressure. The cell was maintained at 150°C.

RESULTS AND DISCUSSION

RhNaX Carbonylation

Figures 1A and B are the spectra of the RhNaX catalyst before and after carbonylation. Spectrum A is simply the untreated RhNaX, while spectrum B is after carbonylation at 120°C with flowing CO at 30 psig for 10 h. IR bands develop slowly at 2096, 2016, and 1831 cm^{-1}.

The two bands at higher wavenumber values are assigned to Rh(I)(CO)$_2$–NaX; this species is well established in the literature (*5, 8, 25*). Also, the broad, weak band at 1831 cm^{-1} suggests the presence of a multinuclear species, Rh$_x$(CO)$_y$.

It is important to note here that we have formed the dicarbonyl on NaX without drying the zeolite (vide infra). Yamanis and Yang (*8*) and Andersson and Scurrell (*25*) report that heating the catalyst in oxygen or nitrogen prior to CO absorption also yields the dicarbonyl.

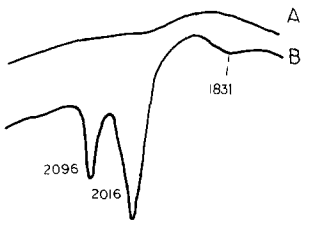

FIG. 1. RhNaX (preparation G with 1% Rh). (A) Untreated, (B) after 12 h with 30 psig CO at 120°C.

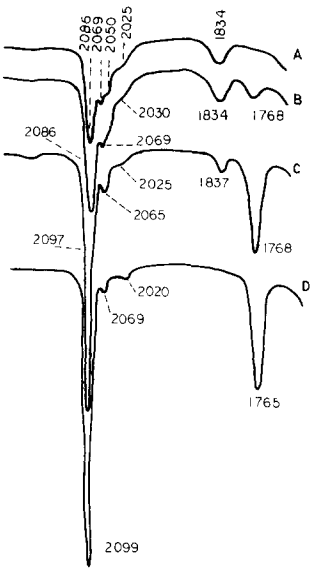

FIG. 2. RhNaY (1% Rh) with 30 psig CO and heating to 120°C. Temperatures: (A) 95°C, (B) 110°C, (C) 120°C for 3 h, (D) 120°C for 10 h. No further spectral changes occur after 10 h.

RhNaY Carbonylation

Carbonylation of RhNaY with 30 psig flowing CO while heating to 120°C is more complex than the carbonylation of RhNaX. In Fig. 2 a set of IR spectra taken during carbonylation as a function of time and temperature are shown. Spectrum A, taken at 95°C, shows weak bands at 2069, 2050, 2025, and 1834 cm^{-1} and a sharp band at 2086 cm^{-1}. Upon heating the catalyst to 110°C, the region 2070–2020 cm^{-1} shows better resolution and a new band at 1768 cm^{-1} appears. The band at 1768 cm^{-1} continues to grow in intensity with further heating of the sample. At the same time the band at 1834–1837 cm^{-1} disappears. After 10 h, no further spectral changes are observed. The final spectrum has bands at 2099s, 2069w, 2020w, and 1765m cm^{-1} (Fig. 2D).

It is evident that several rhodium carbonyl species are formed during carbonyla-

TABLE 1

Values for Various Rhodium Carbonyls

Complex	Support	ν_{CO} (cm^{-1})	Reference
$Rh_6(CO)_{16}$	Nujol	2075s, 2025w, 1800m	*27*
$Rh_6(CO)_{16}$	NaX[a]	2082s, 2040w, 2000wsh, 1805s	*19*
$Rh_6(CO)_{16}$	Silica	2080, 1800	*16*
$Rh_6(CO)_{16}$	Alumina	2065, 1804	*17*
$Rh_6(CO)_{16}$	NaY	2095vs, 2045, 2020, 1764s	*26*
$Rh_6(CO)_{16}$	NaY	2095vs, 2080sh, 2060w, 1765s	*15*
$Rh_6(CO)_{16}$	NaY	2099vs, 2069, 2020, 1765s	This work
$Rh_4(CO)_{12}$	Silica	2076, 2046, 1881–1870[b]	*16*
$Rh_4(CO)_{12}$	Alumina	2068, 1840	*16*
$Rh_4(CO)_{12}$	NaY	2086, 1834	This work
Rh(III)CO	NaY	2172	*18*
$Rh(CO)_2$	NaX	2046, 1987	*19*
$Rh(CO)_2^+$	NaX	2099, 2017	*19*
$Rh(CO)_2^+$	NaX	2085, 2014	*7*
$(Rh(CO)_2Cl)_2$	KBr	2105, 2089, 2035, 2003	—
$Rh(CO)_2O_zH_2O$	NaY	2116, 2048	*20*
$Rh(CO)_2(O_z)_2$	NaY	2101, 2022	*20*
$Rh(CO)_2^+$	NaY	2110, 2096, 2047, 2022	This work
$Rh(CO)_2^+$	NaX	2096, 2016	This work

[a] $Rh_6(CO)_{16}$ on the surface of NaX.

[b] Variation in the bridging carbonyl stretching frequency observed with the CO pressure applied during $Rh_4(CO)_{12}$ adsorption.

tion. Ultimately, $Rh_6(CO)_{16}$–NaY is generated. The infrared spectrum for this species (Fig. 2D) is in excellent agreement with results reported by Mantovani *et al.* (*15*) and Gelin *et al.* (*26*). (For a direct comparison, see Table 1.) Assignment of the spectrum observed in Fig. 2D to $Rh_6(CO)_{16}$ requires significant shifts of the bands observed for free $Rh_6(CO)_{16}$ and $Rh_6(CO)_{16}$ on the surface of NaX. For example, the bridging carbonyl shifts 40 cm^{-1}. This has been taken to be evidence that the $Rh_6(CO)_{16}$ resides in the supercage (*12*). Theolier *et al.* (*16*) deposited $Rh_4(CO)_{12}$ onto alumina and silica, and obtained IR bands at 2068 and 1840 cm^{-1} for alumina, and 2076, 2046, and 1881–1870 cm^{-1} for silica. Thus, $Rh_4(CO)_{12}$ is a strong candidate for the intermediate giving a bridging carbonyl at 1834 cm^{-1}. This is consistent with the known synthesis of $Rh_6(CO)_{16}$ from $Rh_4(CO)_{12}$ in solution (*28*).

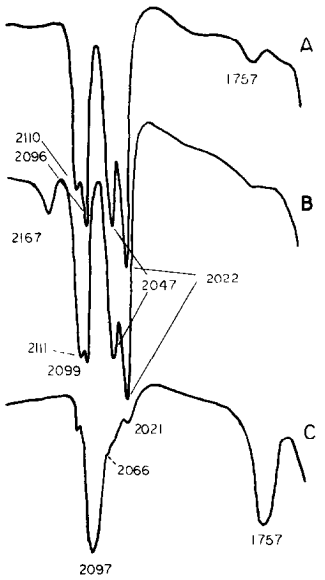

FIG. 3. RhNaY carbonylation. (A) RhNaY ($RhCl_3$ exchange) dried in air prior to CO adsorption, (B) RhNaY (pentaammine chloride exchange) dried in air prior to CO adsorption, (C) (B) not air dried prior to CO adsorption.

It has been proposed by Primet *et al.* (*18*) that the following reactions take place to form $Rh(I)(CO)_2$–NaY:

$$Rh(III) + CO \rightarrow Rh(III)\text{–}CO$$

$$Rh(III)\text{–}CO + 2CO + H_2O \text{ (or OH groups)} \rightarrow Rh(I)(CO)_2 + CO_2 + 2H^+$$

In a separate experiment, Theolier *et al.* (*16*) have proposed equation (1) to produce silica-supported clusters:

$$2Rh(I)(CO)_2 \xrightarrow[(CO_2 + 2H^+)]{H_2O/CO} 2Rh^0(CO)_m \xrightarrow{\text{CO/high } H_2O \text{ conc.}} Rh_4(CO)_{12}$$
$$\downarrow \text{CO/low } H_2O \text{ conc.} \qquad \downarrow 2Rh^0(CO)_m \qquad (1)$$
$$Rh_z(CO)_t \qquad Rh_6(CO)_{16}$$

In this example $Rh(I)(CO)_2$–silica was generated by O_2 oxidation of $Rh_6(CO)_{16}$–silica formed by impregnation of $Rh_4(CO)_{12}$ in hydrocarbon solvent and subsequent decomposition to the higher nuclearity cluster. Our results are consistent with these proposed reactions. Although the presence of Rh(III)–CO and $Rh(I)(CO)_2$ is not obvious in the spectra shown in Fig. 2, they may be obscured by the broad peaks in the region 2200–2000 cm^{-1}.

The important role of the zeolite water is exemplified by the following set of results. When the RhNaY prepared from a rhodium trichloride exchange was heated in air at 190°C for 10 h, the predominant species formed after atmospheric CO adsorption was $Rh(I)(CO)_2$–NaY, as shown in Fig. 3A. The spectrum for this assigned dicarbonyl differs from the $Rh(I)(CO)_2$–NaX in that four absorption bands are present. A similar result was found on RhNaY prepared from the exchange of rhodium pentaammine chloride, as shown in Fig. 3B. These data are in close agreement with Primet *et al.* (*18*). However, if the ammine preparation was carbonylated with 30 psig CO at 120°C without first drying, the $Rh_6(CO)_{16}$–NaY cluster was produced (see Fig. 3C). Thus, by drying the zeolite prior to CO adsorption, the sequence proposed by Theolier *et al.* (*16*) is probably not able to proceed. Without water, Rh(III) may only be reduced to Rh(I).

It has recently been postulated that the four IR bands of $Rh(I)(CO)_2$–NaY represent two types of rhodium dicarbonyl (*20*). The bands at 2101 and 2022 cm^{-1} represent a $Rh(CO)_2(O_z)_2$, where O_z is lattice oxygen, while the bands at 2116 and 2048 cm^{-1} represent a dicarbonyl in which one of the lattice oxygens is replaced by water.

It is now possible to reconcile the different results in the literature. Gelin *et al.* (*9*), Primet *et al.* (*18*), and Arai and Tominaga (*14*) dried their catalysts prior to CO adsorption. Davis *et al.* (*13*) did not dry their catalyst. Immediately before use, Mantovani *et al.* (*15*) dried the rhodium ammine-exchanged zeolite only at room temperature. Therefore, there was sufficient water present to allow cluster formation. At this time, it is not clear why the RhNaX materials do not form clusters in the presence of water.

Rhodium Carbonyl Reactions with Phosphines

In an earlier paper (*19*), it was postulated that the reactions of rhodium carbonyls with different size phospines could distinguish between surface and intrazeolite rhodium carbonyl species. Large phosphines incapable of penetrating the 8-Å pores of the zeolites NaX and NaY can react with surface complexes only. In this work, we used *n*-hexyldiphenylphosphine (HDP) as the large phosphine. Dimethylphenylphos-

phine (DMP) is used to indicate that rhodium carbonyls can react with small phosphines under our experimental conditions.

Figure 4 is a collection of spectra taken after reaction with HDP and DMP. The rhodium dicarbonyl species are shown in Fig. 4A. Spectrum 4B was recorded following the reaction with DMP. The formation of a phosphinated rhodium carbonyl complex is indicated by the 1964-cm^{-1} band. The dicarbonyl species were completely removed. Spectra C shows the reaction of the rhodium carbonyls with HDP. The bands at 2096 and 2023 cm^{-1} are removed as the weak band at 1965 cm^{-1} develops. The bands at 2122 and 2047 cm^{-1} shift to slightly lower wavenumbers but remain intact. Therefore, two types of dicarbonyl species exist on this zeolite. Here we have distinguished the two dicarbonyl species on the basis of their reactivity with HDP. A possible cause of the difference in HDP reactivity is dicarbonyl location (on the surface or within the pore system of the zeolite).

The $Rh(I)(CO_2)$–NaX species reacts with DMP in a similar manner as the two NaY supported dicarbonyls (see Fig. 5B). A weak shoulder at 1990 cm^{-1} develops as the 2095-cm^{-1} band is removed. However, the NaX supported dicarbonyl does not react with HDP (see Fig. 5C). As with one of the dicarbonyl species on NaY, $Rh(I)(CO)_2$–NaX could be located within the pore network of the zeolite.

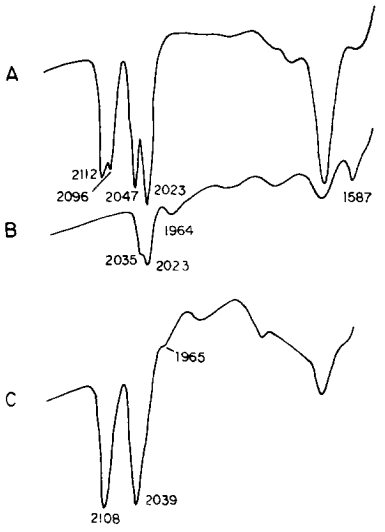

FIG. 4. Rhodium dicarbonyl reactions with phosphines. (A) $Rh(I)(CO)_2$–NaY, (B) (A) following DMP exposure at 150°C, (C) (A) after 7 h with HDP at 150°C.

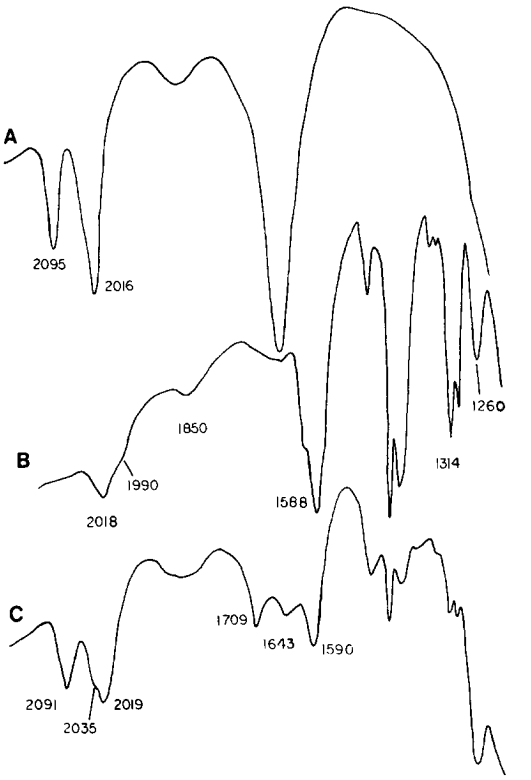

FIG. 5. Rhodium dicarbonyl reactions with phosphines. (A) $Rh(I)(CO)_2$–NaX, (B) (A) following DMP exposure at 150°C, (C) (A) after 12 h with HDP at 150°C.

Figure 6 shows the spectra taken following the reaction of $Rh_6(CO)_{16}$–NaY (Fig. 6B) with DMP and HDP in Figs. 6A and C, respectively. DMP reacts with the $Rh_6(CO)_{16}$ to produce a rhodium carbonyl phosphine complex as indicated by the 1959-cm^{-1} band. The intensities of the 2091 and 2029 cm^{-1} bands suggest the presence of a $Rh(I)(CO)_2$–NaY species also. HDP does not alter the intensity of the $Rh_6(CO)_{16}$ bands. It has been shown previously that $Rh_6(CO)_{16}$ residing on the surface of NaX reacts with a phosphine too large to pene-

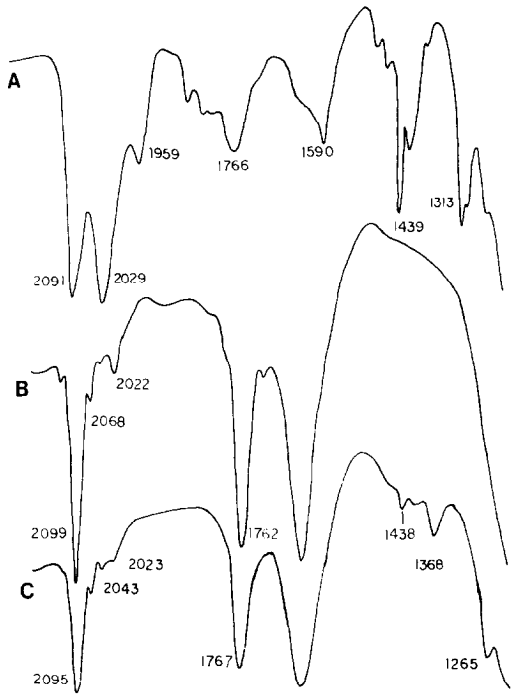

FIG. 6. $Rh_6(CO)_{16}$–NaY exposed to HDP and DMP. (A) (B) following reaction with DMP, (B) $Rh_6(CO)_{16}$–NaY, (C) (B) after contact with HDP.

trate the pores of NaX at 25°C to form rhodium carbonyl phosphine complexes (ν_{CO} = 1963 cm^{-1}) (*19*). Since the IR spectrum of $Rh_6(CO)_{16}$–NaY is not affected by the presence of HDP, the cluster must reside within the supercages of NaY.

RhNaY At Hydroformylation Conditions

Figure 7 shows the spectrum collected from RhNaY at hydroformylation conditions after precarbonylation to form $Rh_6(CO)_{16}$–NaY. Significant spectral changes occur in the three regions bounded by 2150–1750 cm^{-1}, 1750–1600 cm^{-1}, and below 1600 cm^{-1}. These will be referred to as regions I, II, and III, respectively.

In region I, a band at 2042 cm^{-1} develops after 1 h of exposure to reactants. The band at 2021 cm^{-1} becomes more resolved after 5.5 h as shown in Fig. 7B. The entire spectrum does not undergo any further change beyond 20 h of contact with reactants. This time coincides well with the time required to reach steady state in the differential bed reactor (*22*). At 20 h, numerous weak bands appear between 2035 and 1900 cm^{-1}. Notice that the strong bands due to the $Rh_6(CO)_{16}$ (2093, 2067, and 1763 cm^{-1}) do not change appreciably in the presence of reactants.

In region II, three bands develop with time. Adsorbed aldehydes produce a band at 1721 cm^{-1}, which moves to 1691 cm^{-1} at steady state. After 5.5 h, shoulders on the bending mode of water (1640 cm^{-1}) were present. At steady state, these are resolved into bands at 1662 and 1623 cm^{-1}.

Region III is the deformation band region for CH_3, CH_2, and CH groups. Bands at 1455, 1442, and 1380 cm^{-1} in spectrum A are due to adsorbed propylene. After 5.5 h, these bands are intensified as a result of the accumulation of adsorbed products. At steady state, 1463 cm^{-1} has replaced 1455 cm^{-1}, while 1290 cm^{-1} has developed.

With the exception of the 1290-cm^{-1} peak, all bands in region III are attributable

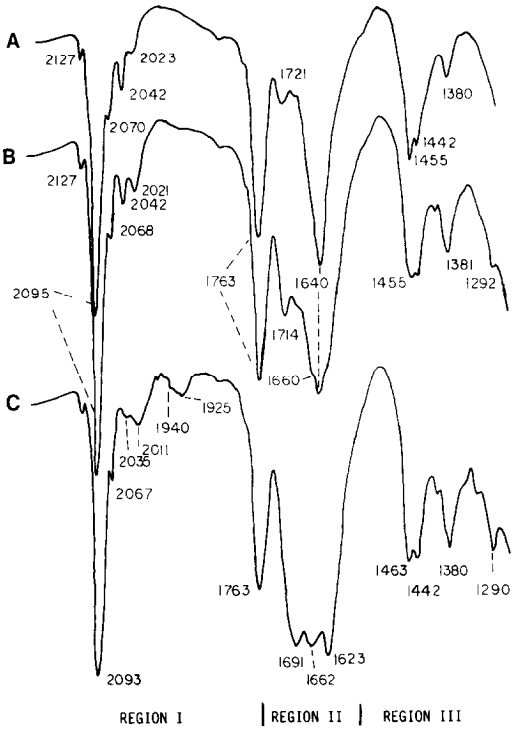

FIG. 7. RhNaY (1% Rh) under hydroformylation conditions. (A) After 1 h, (B) after 5.5 h, (C) at steady state (20 h).

to either adsorbed product or adsorbed propylene. These have been confirmed via comparison of spectra resulting from adsorption of aldehydes and propylene onto plain NaY (*24*). The 1290-cm^{-1} band has been assigned to the rocking deformation mode of a rhodium alkyl species. The rhodium is bonded to the central carbon of a propyl group. This assignment is supported by the fact that similar band displacements occur for a methylene group adjacent to a metal (*29*).

The assignment of the 1660-cm^{-1} band is difficult since several species are likely candidates. It has been proposed that the rate-determining step of the homogeneous, rhodium carbonyl, hydroformylation mechanism is the hydrogenolysis of the acyl complex. If this is correct, then it is expected that the acyl concentration would be higher than other intermediates. The metal acyl has been identified by a decrease of the carbonyl stretching frequency from its position in ketones. IR values for an acyl complex have been reported in the range from 1720 to 1650 cm^{-1} as shown in Table 2. The assignment is not clear as seen by the scatter in Table 2. Generally, it has been assigned at either one of two positions; at 1725–1720 and at 1675–1650 cm^{-1}. Another species which adsorbs at approximately 1660 cm^{-1} is an α, β-unsaturated aldehyde.

TABLE 2

Values for Acyl Carbonyl Frequencies

Compounds	ν_{CO} (cm^{-1})	Reference
$(NEt_4)(Rh_6(CO)_{15}(COPr)$	1655–1670	*30*
$Rh(COCH_3)$ I–NaX	1720	*8*
CH_3CO $Mn(CO)_5$	1661	*31*
NaX–$ORh(COCH_3)I$	1724	*32*
$(C_8H_{17}CO)Co(CO)_4$	1720	*33*
$(CH_3CO)Co(CO)_4$	1720	*34*
$(nBuCO)Co(CO)_4$	1720	*34*
M–CO–X[a]	1640	*35*
C_2H_5CO $Ir(CO)_3P$–i–Pr_3	1671	*36*
$(C_2H_5CO)Co(CO)_3PBu_3$	1676	*36*

[a] X = halide.

TABLE 3

Carbonyl Band Positions for Aldehydes and Ketones (*37*)

	ν_{CO} (cm^{-1})
Aldehydes	
Formaldehyde	1754, 1724
Acetaldehyde	1730
Propionaldehyde	1724
Valeraldehyde	1695
Ketones	
Methyl propyl ketone	1694
Methyl ethyl ketone	1730
Ethyl ketone	1724
Ethyl propyl ketone	1695

Such a compound would be formed from an aldol condensation reaction between two aldehydes with subsequent dehydrogenation. 2-*trans*-Hexenal was adsorbed onto NaY to approximate the aldol condensation products, and gave a band at 1680 cm^{-1}. Therefore, the dehydrogenated aldol condensation products are unlikely to be the source for the 1660-cm^{-1} band. Since no other products of the hydroformylation reaction absorb in this region, the band at 1660 cm^{-1} is tentatively assigned to the rhodium acyl, Z–O–$Rh(COPr)L_2$, where Z = zeolite, and L = CO or O_z. Additional reasons for this assignment follow.

Another argument in favor of our acyl assignment is by use of the analogy to aldehyde and ketone carbonyl band positions. In Table 3, values for ν_{CO} are shown as a function of alkyl group size. Note that there exists a 36-cm^{-1} shift in the stretching frequency between methyl propyl ketone and methyl ethyl ketone. A 29-cm^{-1}shift is observed between diethyl ketone and ethyl propyl ketone. Additionally, the carbonyl band position changes 35 cm^{-1} on going from acetaldehyde to pentanal. By changing the olefin at hydroformylation conditions, the acyl would occur at different positions. The steady-state spectrum for RhNaY (1% Rh) (denoted catalyst C in our

accompanying report) at ethylene hydroformylation conditions contains a 1700-cm^{-1} band, but not one at 1660 cm^{-1}. This 1700-cm^{-1} band is tentatively assigned to the rhodium acyl for propionaldehyde production.

Finally, the behavior of a catalyst prepared without NaCl in the exchange slurry at pH 4 provides another argument for the acyl band assignment. This catalyst initially was active, but deactivated after several hours. As shown in Fig. 8, the acyl intermediate appears earlier than for catalyst C, but then is absent at 4.5 h. If the band at 1660 cm^{-1} were from an adsorbed product, the band would not completely disappear after 4.5 h. This is due to the strong adsorption of oxygenated products on the zeolites. Complete desorption of oxygenated products is not possible even at temperatures around 200°C.

Attempts to remove the 1660 cm^{-1} by replacing reactants with CO/H_2 for catalyst C as well as other stable catalysts did not alter the band intensity or position. This is taken as indirect evidence for the stability of the acyl.

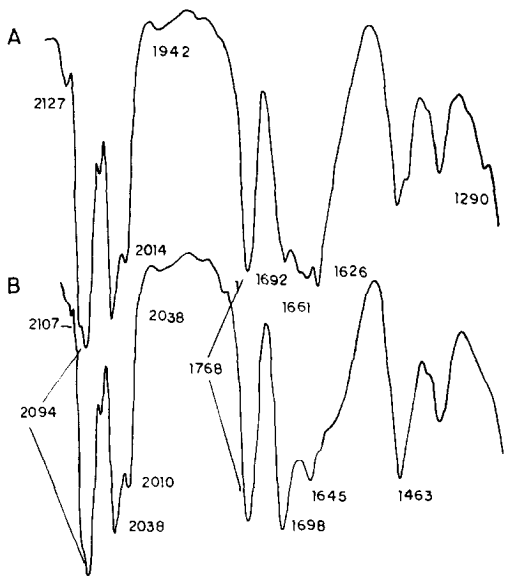

FIG. 8. Catalyst prepared at pH 4 without NaCl in the exchange slurry under hydroformylation conditions. (A) after 0.5 h, (B) after 4.5 h.

Olefin interaction with a large cation shifts the double-bond stretch to a lower frequency. It has been shown that propylene adsorbed on NaY produces a band at 1630 cm^{-1} (*38*). Based on this value, we have assigned the 1623-cm^{-1} peak to Na^+–propylene interaction. Rhodium carbonyl interaction with Lewis acid sites on the zeolite also could produce a band as low as 1600 cm^{-1}. No shift is seen for the band at 1623 cm^{-1} when ^{12}CO is replaced with ^{13}CO, while all other bands assigned to rhodium carbonyls shift to lower wave numbers.

The bands in region I are attributable to rhodium carbonyl species. However, positive assignments to specific complexes for all of these bands are not possible. As discussed above, the position of the dicarbonyl bands are dependent upon the ligands on the Rh. We have assigned the band at 2042 cm^{-1} (Fig. 7A) to the structure

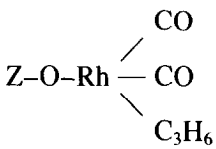

When $Rh_6(CO)_{16}$–NaY is exposed to propylene and CO at 150°C, a band at 2042 cm^{-1} develops initially. After 20 h, this band moves to 2037 cm^{-1}. Identical changes occur in spectrum under reaction conditions (Figs. 7A–C). Lefebvre and Ben Tarrit (*20*) also show that a similar complex can be formed with ethylene producing bands at 2110 (sym) and 2042 cm^{-1} (asym). The symmetric stretch in our spectrum is probably obscured by the 2093-cm^{-1} band of the $Rh_6(CO)_{16}$. In a homogeneous study, a $Rh(C_2H_5)(CO)_4$ complex was identified via IR by its bands at 2115, 2037, and 2019 cm^{-1} (*31*). The remaining bands in region I are believed to be rhodium carbonyl intermediates. Batch isotopic labeling experiments (^{13}CO–^{12}CO, D_2–H_2) were not helpful in identifying these bands due to their extreme sensitivity to CO and H_2 partial pressures. A flow *in situ* IR experiment in which D_2 was substituted for H_2 did not produce any

spectral changes. A Rh–D stretch would appear in region III, which has numerous bands present at steady state. Labeled ^{13}CO flow experiments were cost prohibitive. Thus, we never conclusively identified the presence of Rh–H.

It is illustrative to compare the steady-state positions of the IR bands with those reported in the literature. To date, no heterogeneous data is available. IR stretching frequencies for homogeneous intermediate species with cobalt and rhodium are shown in Table 4. It is noteworthy that IR frequencies seen in this study are similar to those observed in homogeneous catalytic systems. Homogeneous reaction intermediates give bands with values ranging from 1993 to 2114 cm^{-1}. This overlaps closely with those observed on the rhodium zeolite. However, there are no equivalent bands in the homogeneous studies as low as 1920 cm^{-1}.

Comparison of the observed species with the proposed intermediates of the Heck–Breslow mechanism (*42*) reveals that the heterogeneous rhodium carbonyl catalyst could be following the same path as the homogeneous rhodium carbonyl analogue. Those species which are not observed are the hydrido-rhodium species, and the coordinated olefin. Absence of IR bands for these species is not surprising considering their position in the catalytic cycle. The coordinated olefin to metal alkyl transition would be fast at 150°C. This reaction consumes one hydrido species. The oxidative addition of H_2 prior to aldehyde elimination is believed to be the rate-determining step.

TABLE 4

Carbonyl Band Positions for Hydroformylation Intermediates

	ν_{CO} (cm^{-1})	Reference
$HCO(CO)_4$	2114, 2053, 2032, 1993	*39*
$RCo(CO)_3$	2105, 2035, 2018	*40*
$MeCo(CO)_4$	2105, 2036, 2109	*34*
$RCOCo(CO)_3$	2108, 2010	*40*
$RCOCo(CO)_4$	2103, 2044, 2022, 2003, 1720	*34*
$RRh(CO)_4$	2115, 2037, 2020	*41*

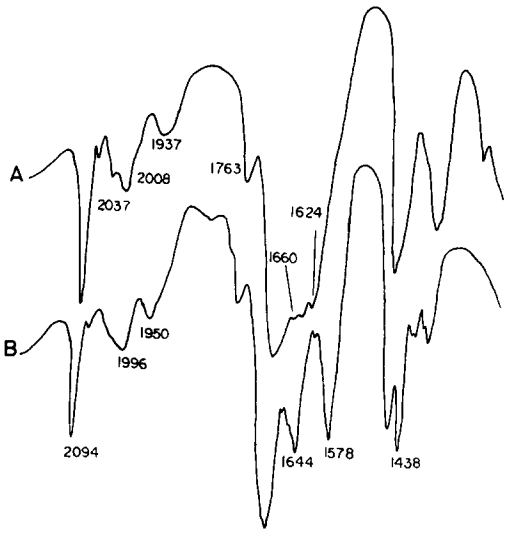

FIG. 9. RhNaY (1% Rh) under hydroformylation conditions. (A) At steady state, (B) with HDP after 7 h.

Therefore, this dihydride would have a relatively short life span as well. There is evidence for the alkyl and acyl species, both of which implies the presence of hydride complexes.

The partial pressure dependencies of propylene, CO, and H_2 on the hydroformylation rate (*22*) provide additional evidence for the similarities between the homogeneous and heterogeneous mechanisms. The results presented in our accompanying paper correspond to homogeneous data. Based on the similarities of reaction intermediates and partial pressure dependencies, it is concluded that our heterogeneous rhodium catalysts react through a mechanism similar to that observed in solution.

Active Site Location

The reactivity of the reaction intermediate, rhodium carbonyls with HDP, was used as a probe to determine the location of the active site. The catalyst RhNaY (1% Rh) was allowed to reach steady state as shown in Fig. 9A. After 7 h in contact with HDP, spectrum B was taken. Notice that the bands assigned to various intermediates are removed. Specifically, the rhodium alkyl bands at 2037 and 1292 cm^{-1}, the acyl at

1660 cm^{-1}, and the adsorbed propylene at 1623 cm^{-1} are not present following the HDP exposure. As discussed in our accompanying report (*22*), injection of HDP altered the activity of this catalyst. These results are consistent with hydroformylation taking place on the external surface of the zeolite. Note also that the $Rh_6(CO)_{16}$ bands were not altered by HDP.

Figure 10 is a collection of the steady-state IR for catalyst C which had been pretreated differently. The pretreatments were N_2, air dried, and precarbonylated as shown in Figs. 10A,B,C, respectively. It is evident that pretreatment had little effect on the final spectra. This is not surprising since these pretreatments had no effect on catalytic activity (*22*). Note that all three spectra contain $Rh_6(CO)_{16}$ bands at 2095 and 1763 cm^{-1} in varying intensities. Since spectrum C indicates that $Rh_6(CO)_{16}$ is the most abundant species, and from (*22*) the activity of this catalyst is reported to be essentially the same as with other pretreatments suggest that the cluster is not the active site for the hydroformylation of propylene. Rather, it appears that it is merely a rhodium sink. This does not preclude the possibility that the clusters may act as a rhodium source by decomposition under H_2. (H_2 added to $Rh_6(CO)_{16}$–NaY decomposes the cluster to the dicarbonyl.) Recall that the partial pressure of H_2 is three times that of CO. Because of this large amount of rhodium occupied in the cluster, it is apparent that only a small fraction of the metal is involved in catalysis. Hence, the combination of catalytic activity and *in situ* FTIR studies leads to the conclusion that the rhodium utilization is poor for hydroformylation at 1 atm total pressure.

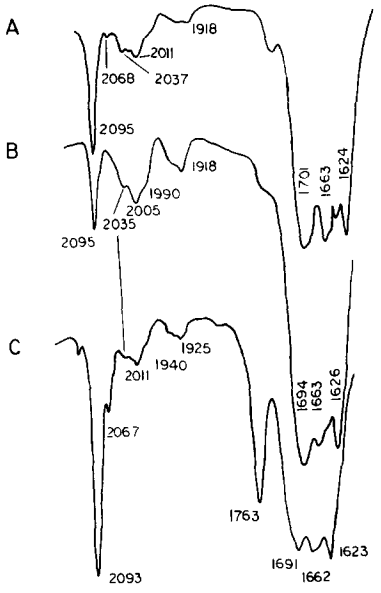

FIG. 10. RhNaY (1% Rh) at steady state with differentiation pretreatments. (A) N_2 heated to 120°C, (B) air-dried, (C) precarbonylated.

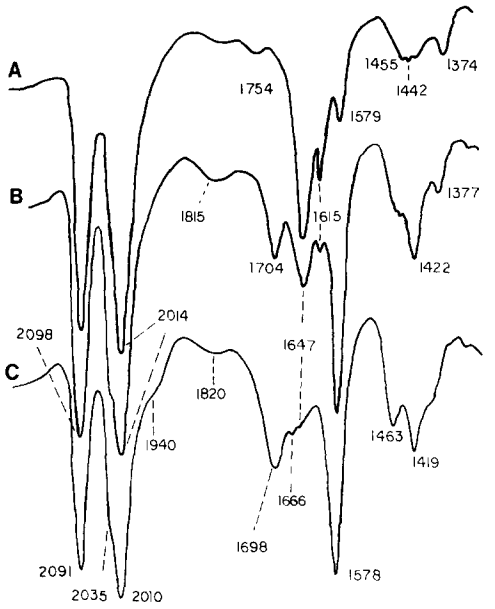

FIG. 11. Catalyst G under hydroformylation conditions. (A) After 5 min, (B) after 1 h, (C) after 26 h.

RhNaX under Hydroformylation Conditions

Figure 11 is a collection of spectra taken of catalyst G under reaction conditions. The RhNaX does not lend itself to the same detailed analysis as performed on RhNaY because the positions of the dicarbonyl bands, 2098 and 2014 cm^{-1}, obscure the region 2035–1950 cm^{-1}. However, other important features are present. Shoulders on the high-frequency sides of the dicarbonyl

bands at 2100 and 2035 cm^{-1} are present suggesting the presence of the rhodium alkyl. The broad shoulder at 1940 cm^{-1} in spectrum C overlaps the region where many reaction intermediate bands are present on RhNaY. The band at 1666 cm^{-1} indicates the presence of the rhodium acyl complex. The 1615-cm^{-1} band is to large of a shift for Na^+–propylene double-bond interaction. ^{13}CO substitution shifted the 1615-cm^{-1} band to 1600 cm^{-1}, indicating that it is a carbonyl band. Specific assignment of this carbonyl has not been made.

Aldehyde adsorption onto NaX is considerably different on NaY due to the difference in silica and alumina content. Over time, a shift in aldehyde band is observed, although the initial band is 1704 cm^{-1}. The band is not as intense as on NaY. This is due to adsorption of *n*-butyraldehyde in a carboxylate fashion. Bands at 1578 and 1419 cm^{-1} are due to the asymmetric and symmetric stretch of the carboxylate group

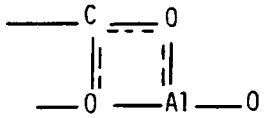

Chapman and Hair (*43*) performed IR adsorption studies with benzaldehyde on silica, alumina, and silica–alumina at various compositions. Only the alumina-rich material allowed this type of adsorption. On silica, no carboxylate bands appeared.

RhNaX vs RhNaY

In our previous work (*13*), we postulated that rhodium on zeolites NaX and NaY were conducting the hydroformylation reaction in a similar fashion although the before and after IR of the two catalysts were different. The present work supports this postulate (compare spectra C in Figs. 11 and 7). Each catalyst indicates the presence of rhodium alkyl and acyl complexes. A direct comparison of the region 2050–1900 cm^{-1} is not possible, although the broad shoulder at 1940 cm^{-1} on catalyst RhNaX suggests the presence of similar intermediates. Based on these observations, it is believed that the zeolite (NaX or NaY) is not altering the reaction mechanism.

Since the hydroformylation startup, regioselectivity, and activation energies are nearly the same for catalysts RhNaX and RhNaY, it is postulated that the active species for hydroformylation is the same for each catalyst. Although no Rh–H band was observed by IR, it is believed that the active species contains a hydride because of what is known from homogeneous systems. The following reactions are postulated to give the active species:

$$Rh(CO)_2\text{–}NaX \rightleftarrows HRh(CO)_x\text{–}NaX + H^+\text{–}NaX$$

$$Rh_6(CO)_{16}\text{–}NaY \rightleftarrows Rh(CO)_2\text{–}NaY \rightleftarrows HRh(CO)_x\text{–}NaY$$

It was not possible to determine accurately whether the $Rh_6(CO)_{16}$–NaY or the $Rh(CO)_2$–NaX were decomposing to form the active sites. Transmission through the wafer decreased as the zeolite saturated with products. Therefore, a simple comparison of the before and after spectra is not possible. The equations for hydride formation are written as equilibria. Although the partial pressure of H_2 is three times that of CO, the total pressure may not be high enough to drive the equilibria toward the large production of hydride.

CONCLUSIONS

The present work has shown that *in situ* FTIR spectroscopy is an invaluable tool for elucidating intrazeolite rhodium chemistry. Data was presented showing the role of water in the formation of polynuclear rhodium carbonyls. The combination of catalytic activity and *in situ* FTIR show that a small percentage of the rhodium is involved in the hydroformylation of propylene. FTIR studies support the conclusion that RhNaX and RhNaY undergo similar reaction pathways during the hydroformylation of propene. Finally, these catalysts appear to hydroformylate propylene by homogeneous-like

processes, and for RhNaY the catalysis appears to be occurring on the surface of the zeolite.

ACKNOWLEDGMENTS

Financial support of this work was provided by the National Science Foundation under Grant CPE-8216296, and by the Petroleum Research Fund administered by the American Chemical Society under Grant 14543-G5. One of us (E.J.R.) thanks The Dow Chemical Company for a doctoral fellowship. We thank Johnson Matthey for a loan of $RhCl_3 \cdot 3H_2O$.

REFERENCES

1. Nefedov, B. K., Shutkina, E. M., and Eidus, Ya. T., *Izv. Akad. Nauk SSSR, Ser. Khim.* No. 3, 726 (1975).
2. Nefedov, B. K., Sergeeva, N. S., Zueva, T. V. Shutkina, E. M., and Eidus, Ya. T., *Izv. Akad. Nauk SSSR, Ser. Khim.* No. 3, 582 (1976).
3. Christensen, B., and Scurrell, M. S., *J. Chem. Soc. Faraday Trans. 1* **73,** 2036 (1977).
4. Christensen, B., and Scurrell, M. S., *J. Chem. Soc. Faraday Trans. 1* **74,** 2313 (1978).
5. Scurrell, M. S., and Howe, R. F., *J. Mol. Catal.* **7,** 535 (1980).
6. Andersson, S. L. T., and Scurrell, M. S., *J. Mol. Catal.* **18,** 375 (1983).
7. Yamanis, J., Lien, K. C., Caracotsios, M., and Powers, M. E., *Chem. Eng. Commun.* **6,** 355 (1981).
8. Yamanis, J., and Yang, K. C., *J. Catal.* **69,** 498 (1981).
9. Gelin, P., Ben Taarit, Y., and Naccache, C., *in* "New Horizons in Catalysis" (T. Seiyama and K. Tanabe, Eds.), Vol. 7, p. 898. Elsevier, Amsterdam, 1981.
10. Yashima, Y., Orikasa, Y., Takahashi, N., and Hara, N., *J. Catal.* **59,** 53 (1979).
11. Takahashi, N., Orikasa, Y., and Yashima, T., *J. Catal.* **59,** 61 (1979).
12. Gelin P., Lefebvre, F., Elleuch, B., Naccache, C., and Ben Taarit, Y., *in* "Intrazeolite Chemistry" (G. D. Stucky and F. G. Dwyer, Eds.). Amer. Chem. Soc., Washington, D.C., 1983.
13. Davis, M. E., Rode, E. J., Taylor, D., and Hanson, B. E., *J. Catal.* **86,** 67 (1984).
14. Arai, H., and Tomminaga, H., *J. Catal.* **75,** 188 (1982).
15. Mantovani, E., Palladino, N., and Zanabi, A., *J. Mol. Catal.* **3,** 285 (1977–78).
16. Theolier, A., Smith, A. K., Leconte, M., Basset, J. M., Zanderighi, G. M., Psaro, R., and Ugo, R., *J. Organomet. Chem.* **191,** 415 (1980).
17. Smith, A. K., Hugues, F., Theolier, A., Basset, J. M., Ugo, R., Zanderighi, G. M., Bilhow, J. C., Bilhou-Bougnol, V., and Graydon, W. F., *Inorg. Chem.* **18,** 3104 (1979).
18. Primet, M., Vedrine, J. C., and Naccache, C., *J. Mol. Catal.* **4,** 411 (1978).
19. Hanson, B. E., Davis, M. E., Taylor, D., and Rode, E., *Inorg. Chem.* **23,** 52 (1984).
20. Lefebvre, F., and Ben Taarit Y., *Nouv. J. Chem.* **8**(6), 387 (1984).
21. Shannon, R. D., Vedrine, J. C., Naccache, C., and Lefebvre, F., *J. Catal.* **88,** 431 (1984).
22. Rode, E. J., Davis, M. E., and Hanson, B. E., **96,** 563 (1985).
23. Hicks, R. F., Kelher, C. S., Savatsky, B. J., Hecker, W. C., and Bell, A. T., *J. Catal.* **71,** 216 (1981).
24. Rode, E. J., Ph.D. dissertation. Virginia Polytechnic Institute and State University, Blacksburg, Va., 1985.
25. Andersson, S. C. T., and Scurrell, M. S., *J. Catal.* **59,** 356 (1979).
26. Gelin, P., Ben Taarit, Y., and Naccache, C., *J. Catal.* **59,** 357 (1979).
27. Beck, W., and Lottes, K., *Chem. Ber.* **94,** (1961).
28. Chini, P., and Martinengo, S., *Inorg. Chim. Acta* **3,** 315 (1969).
29. Socrates, G., "Infrared Characteristic Group Frequencies." Wiley, New York, 1980.
30. Chini, P., Martinengo, S., and Garlaschelli, G., *J. Chem. Soc. Chem. Commun.* 709 (1972).
31. King, R. B., King, Jr., A. D., Igbal, M. Z., and C. C. Frazier, *J. Amer. Chem. Soc.* **100,** 1687 (1978).
32. Huang, T., Schwartz, J., and Kitajima, N., *J. Mol. Catal.* **22,** 389 (1984).
33. Whyman, R., *J. Organomet. Chem.* **81,** 97 (1974).
34. Marko, V. L., Bor, G., Almasy, G., and Szabo, P., *Brenn. Chem.* **44,** 58 (1963).
35. Collman, J. P., and Hegedus, L. S., "Principles and Applications of Organotransition Metal Chemistry," University Science Books, Mill Valley, Calif., 1980.
36. Whyman, R., *J. Organomet. Chem.* **94,** 303 (1975).
37. Grasselli, J. G., Ed., "Atlas of Spectral Data and Physical Constants for Organic Compounds." CRC Press, Cleveland, 1983.
38. Forster, H., and Seebode, J., *Zeolite* **3,** 63 (1983).
39. Bor, G., *Inorg. Chim. Acta* **1,** 81 (1967).
40. Alemdaroglu, N. H., Penninger, J. L. M., and Otlay, E., *Monatsh. Chem.* **107,** 1153 (1976).
41. King, R. B., Jr., King, A. D., and Igbal, M. Z., *J. Amer. Chem. Soc.* **101,** 4893 (1979).
42. Pino. P., F. Piacenti, and Bianchi, M., *in* "Organic Synthesis via Metal Carbonyls" (I. Wender and P. Pino, Eds.). Wiley, New York, 1977.
43. Chapman, I. D., and Hair, M. L., *in* "Proceedings, 3rd International Congress on Catalysis, Amsterdam, 1964," p. 408. Wiley, New York, 1965.